Journal of Power Sources 192 (2009) 376–380

Contents lists available at ScienceDirect

Journal of Power Sources

journal homepage: www.elsevier.com/locate/jpowsour

Short communication

In-fibre Bragg grating sensors for distributed temperature measurement in a polymer electrolyte membrane fuel cell

Nigel A. David*, Peter M. Wild, Jingwei Hu, Nedjib Djilali

Department of Mechanical Engineering, University of Victoria, Canada

ARTICLE INFO

Article history:
Received 25 January 2009
Received in revised form 5 March 2009
Accepted 6 March 2009
Available online 19 March 2009

Keywords:
Fibre Bragg grating
Polymer electrolyte membrane fuel cell
Temperature

ABSTRACT

A new application of in-fibre Bragg grating (FBG) sensors for the distributed measurement of temperature inside a polymer electrolyte membrane fuel cell is demonstrated. Four FBGs were installed on the lands between the flow channels in the cathode collector plate of a single test cell, evenly spaced from inlet to outlet. *In situ* calibration of the FBG sensors against a co-located micro-thermocouple shows a linear, non-hysteretic response, with sensitivities in good agreement with the expected value. A relative error of less than 0.2 °C over the operating range of the test cell (~ 20–80 °C) was achieved, offering sufficient resolution to measure small gradients between sensors. While operating the fuel cell at higher current densities under co-flow conditions, gradients of more than 1 °C were measured between the inlet and outlet sensors. Due to their small thermal mass, the sensors also exhibit good temporal response to dynamic loading when compared with the thermocouple. Design and instrumentation of the graphite collector plate features minimal intrusion by the sensors and easy adaptation of the techniques to bipolar plates for stack implementation.

1. Introduction

Heat and water management are two of the most critical determinants of PEM fuel cell performance and have consequently been the subject of numerous experimental and theoretical studies [1–5]. Progress in fully controlling heat and water transport has been limited by the coupling of the processes, lack of understanding of some of the underlying mechanisms, and limitations of experimental techniques. Recent multi-physics computational models have provided significant insight, but their predictive capabilities are not entirely established due to the limited availability of *in situ* experimental measurements [5].

Measurement of the temperature distribution inside an operating fuel cell has been reported by a handful of groups using methods involving electrical based microsensors and optical techniques. Wilkinson and coworkers used a series of micro-thermocouples embedded in the graphite collector plate of a single test fuel cell to measure the temperature at the interface of the gas diffusion layer (GDL) and the graphite plate [6]. They demonstrated this as a useful technique for indirectly mapping the current density across the active area of cell, but only half of their sensors were operational during the experiments due to the fragility of the fine leads.

Micro-fabricated thin film thermistor based temperature sensors were demonstrated by He et al. for measuring the temperature inside a PEM bilayer [7]. The 16 μm thick and 0.25 mm^2 sensors were positioned at the reactant inlet and outlet, and showed a linear response *in situ*, even as the membrane swelled from hydration. Microsensors for the *in situ* measurement of temperature and humidity in micrometallic fuel cells were demonstrated by Lee et al. [8]. These sensing techniques could be useful for studying fundamental heat transfer in PEM fuel cells, but due to the custom nature of the MEAs and elaborate fabrication processes, their scope of application is limited.

An optical technique that does not require the preparation of a custom MEA is described by Wang et al. An infrared camera was used to view the anode side of a fuel cell under different operating temperatures and current densities [9]. They report a temperature resolution of less than 0.3 °C with their technique, and were able to clearly observe gradients of up to 5 °C from inlet to outlet at higher current densities. The gradients were attributed to increased current density along the flow path resulting from increased water production at the cathode, hydrating the membrane more towards the outlet.

Wang et al. see this method as a means of locating hot spots (local higher temperature regions); aiding in proper thermal management and, ultimately, to suggest better cell design. This technique is limited in its application, however, as the anode polar plate needs to

* Correspondingauthor at: Department of Mechanical Engineering, University of Victoria, PO Box 3055 STN CSC, Victoria, BC, Canada V8W 3P6. Tel.: +1 250 853 3198; fax: +1 250 721 6323.
E-mail address: nadavid@uvic.ca (N.A. David).

0378-7753/$ – see front matter © 2009 Elsevier B.V. All rights reserved.
doi:10.1016/j.jpowsour.2009.03.021

be modified with a barium fluoride window, allowing it to be transparent to infrared light for camera viewing. It can, therefore, only be applied to a single cell, or an end cell of a stack. Optical access into a PEM fuel cell is also required in the technique recently developed by Basu et al. [10]. They use tunable diode laser absorption spectroscopy to measure water partial pressure and temperature along individual flow channels of a prototype cell. The temperature measurements however, are not sufficiently accurate nor spatially well resolved for the detailed study of temperature distribution inside a fuel cell.

In this paper, fibre-optic based measurements are presented based on a novel application of in-fibre Bragg grating (FBG) sensors. The use of FBGs is particularly well suited for *in situ* measurements. Optical fibres are not only sufficiently small for minimal impact on cell performance, but when coated with polyimide FBGs are immune to moisture and the electrochemically active environment found inside the cell. In addition, being optical devices, they are inherently insensitive to electromagnetic interference.

2. In-fibre Bragg grating sensing principle

A FBG typically consists of a short segment of single mode optical fibre with a photoinduced periodically modulated index of refraction. See Fig. 1(a). When the grating is illuminated with broadband light, the reflected power spectrum has structure caused by interference of the light with the planes of the grating, much like Bragg diffraction. See Fig. 1(b). The peak of the spectrum in this case occurs at a wavelength corresponding to twice the optical path length between adjacent planes, and is called the Bragg wavelength, $\lambda_B = 2\Lambda n$, where n is the index of refraction of the silica fibre and Λ is the grating pitch. When the grating is subjected to mechanical or thermal strain its pitch changes, causing a shift in the Bragg wavelength.

This shift is given by

$$\frac{\Delta\lambda_B}{\lambda_B} = (1 - Pe)\varepsilon + [(1 - Pe)\alpha + \xi]\Delta T, \quad (1)$$

where Pe is the photo-elastic constant of the fibre, ε is the mechanical strain induced in the fibre, α is the coefficient of thermal expansion of the optical fibre, and ξ is the thermo-optic coefficient.

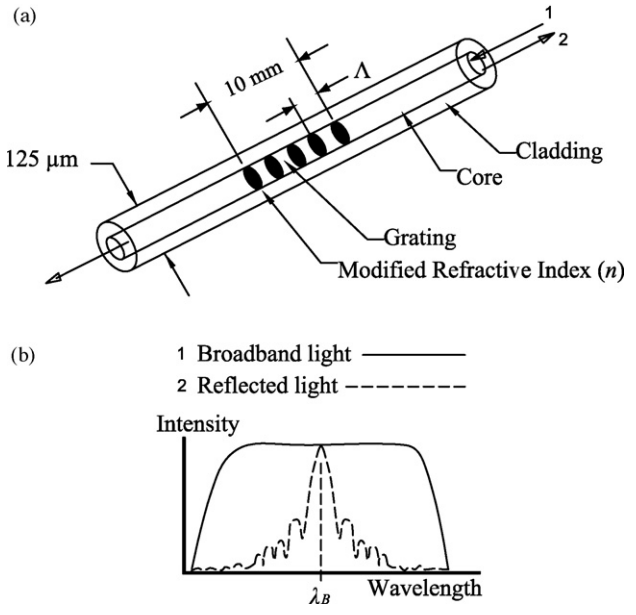

Fig. 1. Schematic of an in-fibre Bragg grating sensor.

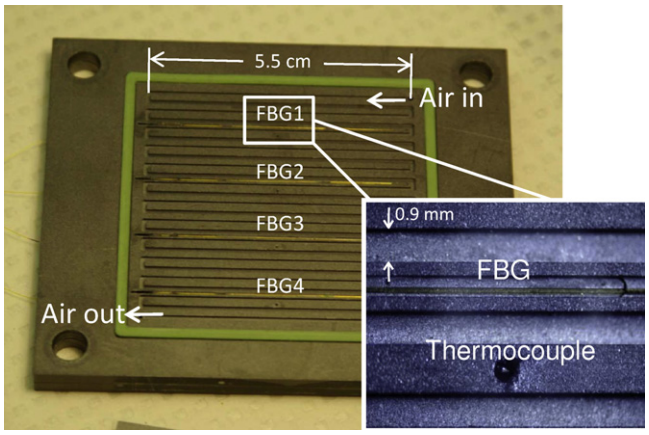

Fig. 2. Graphite bipolar plate with four FBG sensors.

A comprehensive review of FBGs, along with a description of many of their important applications can be found in Rao [11].

3. Experimental setup

3.1. Instrumentation

The FBGs used in this work are 10 mm long, with a nominal room temperature Bragg wavelength of 1550 nm. These are available for purchase from Micron Optics, Inc., Atlanta, GA (model os1100). The standard single mode fibre on to which they are written is 125 μm in diameter and is coated with a thin polyimide layer for durability. The FBG data for calibration and *in situ* measurements is collected with a Micron Optics, Inc. sm130 interrogation unit, with a specified wavelength resolution of 0.1 pm at 10 Hz sampling rate.

Four FBGs have been embedded in the lands separating the serpentine flow channels of a custom two-piece graphite cathode plate machined in house. A top view of this plate is shown in Fig. 2. The fibres lie in milled grooves, 150 μm deep, such that they are not compressed when the cell is assembled and clamped. Deeper sections were milled directly underneath the FBGs to eliminate conductive heat transfer with the graphite plate and ensure the temperature measured by the FBGs is more representative of the MEA. A schematic of the instrumentation is shown in Fig. 3(b).

The two major design challenges of instrumenting the FBGs were limiting bending of the fiber as it entered the cell, and isolating it from strain, which could cause unpredictable measurements. To limit bending, an angled hole was drilled at one end of the groove next to the gasket, connecting to a relief channel milled in the graphite backing plate. This is shown in the schematic of Fig. 3(b). In addition to having a sufficiently deep groove for the FBG to lie in without being compressed by the MEA, cyanoacrylate adhesive was used to fix the fibre in place, isolating it from any strain transferred from outside the cell.

A miniature T-type thermocouple with a wire diameter of 0.13 mm from Omega Engineering, Inc. (Stamford, CT) was installed adjacent to the FBGs for their calibration. The thermocouple was inserted into a 300 μm hole drilled perpendicular to the graphite plate and potted in silicone for insulation. As shown in the schematic of Fig. 3, the thermocouple junction lies in the same plane as the FBGs and, therefore, is well situated for calibration purposes and also provides a comparative measurement during *in situ* testing of the fuel cell.

3.2. Test cell

The instrumented graphite plate described above was sized to fit into a pre-existing test fuel cell assembly in our laboratory. The

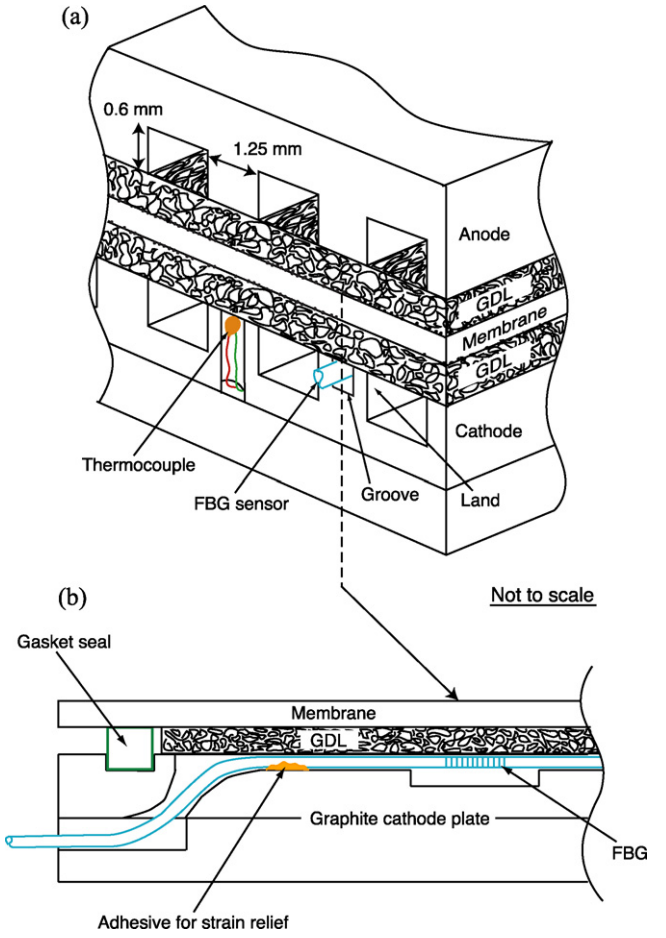

Fig. 3. Schematic of the *in situ* FBG sensor with adjacent thermocouple for calibration (a). The side view schematic in (b) shows how the FBGs were installed into the two-piece graphite cathode plate.

assembly consists of gold plated current collector plates, and stainless steel manifolds for gas distribution and water circulation for the cell heating system. This assembly can be seen in Fig. 4, where the fibre optics are also shown entering the cathode plate.

MEAs for the test cell were fabricated at the National Research Council Institute for Fuel Cell Innovation, Vancouver, Canada. An active area of 30.25 cm^2, with platinum loading of 0.4 $mg/cm^2$was achieved by masking and spray deposition of a carbon catalyst ink onto Nafion © 115 membrane. The GDL used for the MEAs is Toray paper with 10% PTFE content and was hot pressed onto the carbon catalyst.

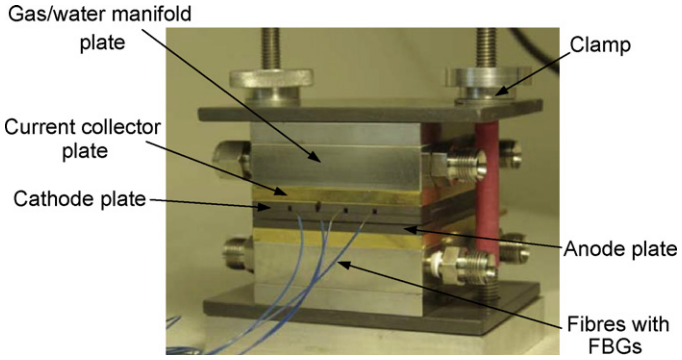

Fig. 4. Photograph of the the single test cell assembly. The cell temperature is set by circulating deionized water from a temperature controlled bath in the test station through the stainless steel plates on either side of the cell.

Table 1
Sensitivities of the four FBG sensors calibrated before and afer experimental testing, 11 days apart.

FBG	Sensitivity ($pm\,°C^{-1}$)	Sensitivity after 11 days
1	10.84	10.76
2	10.73	10.69
3	10.85	10.81
4	10.84	10.79

The test cell is operated using a Ballard 3kW fuel cell test station, which enables the control of the fuel and oxidant flow rate, and the cell temperature with a water heating system. The current density of the fuel cell is varied using an electronic load bank (Dynaload Inc., MCL488, Hackettstown, NJ) that is connected via copper leads to the gold plated collector plates on either side of the single cell. The cell voltage and the thermocouple voltage were measured using analog inputs on a 16 bit data acquisition device (National Instruments Inc.).

4. Experimental methods

4.1. Calibration

Calibration of the four FBGs was routinely carried out before and after acquisition of each data set. The FBGs were calibrated against the thermocouple situated in the same plane as the fibres. See Fig. 3. To reproduce the *in situ* environment, the sensors were covered with a piece of GDL and then clamped between half inch aluminum plates. The high thermal conductivity of aluminum minimizes the potential for thermal gradients within the assembly and allows for thermal cycling in a reasonable amount of time. The assembly was placed in a programmable laboratory convection oven (Cascade Tek Inc., Hillsboro, OR), and cycled between ~ (30–70 °C) at a rate of ~ 0.2 °C/min. Each data point from the thermocouple was taken as the mean value of 100 samples acquired at a rate 1 kHz, resulting in a resolution of approximately ~ 0.05 ° C for these measurements.

4.2. In situ testing

As a baseline case for the *in situ* measurements, the current was set to zero, and only the cell temperature was varied using the water heating system. This was to provide a reference for the temperatures measured by the FBGs while drawing current from the cell with the load bank.

For the case of cell operation, the hydrogen and air were fed into the cell in co-flow mode at a flow rate of 1.0 standard liters per minute and a pressure of 15 psi. The cell was first conditioned at

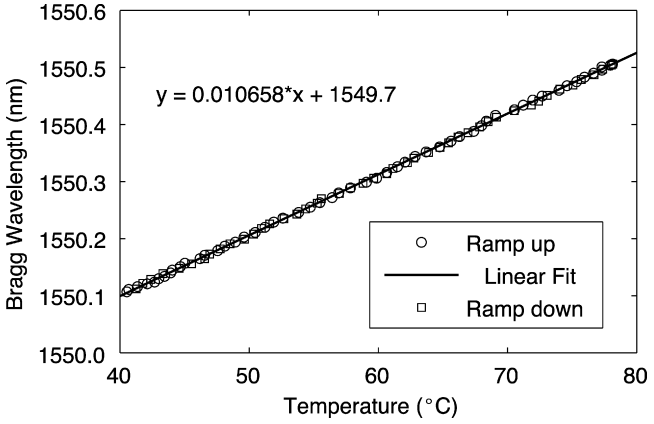

Fig. 5. Calibration data for one of the FBG sensors.

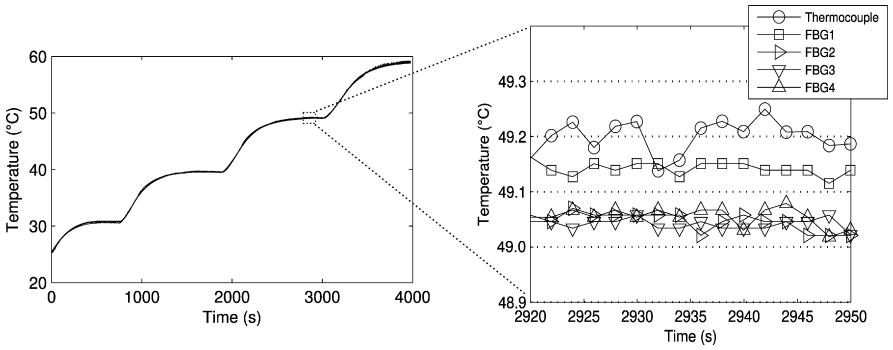

Fig. 6. FBG and thermocouple measurements under varying temperature and zero current conditions.

room temperature with a current density of 0.3 A cm^{-2} for approximately 30 min to humidify the membrane. The current was then increased incrementally like for obtaining polarization curve. During testing, temperature data were taken from the FBGs sensors and the co-located thermocouple every 2 s to gain dynamic information of the temperature profile at the MEA/graphite plate interface inside the cell.

5. Results and discussion

5.1. Calibration

A representative calibration curve for one of the FBGs is presented in Fig. 5 and shows that there is essentially no hysteresis. The sensitivity of this particular FBG was determined to be 10.7 pm °C^{-1}, from a linear fit to the data, which is in good agreement with the literature [11]. There was good agreement between the four sensors, as well as good repeatability; Table 1 shows the sensitivities of all four FBGs measured 11 days apart. By interrogation of the FBGs using the Micron Optics unit, a temperature resolution of 0.01 ° C for the individual FBG sensors was possible.

5.2. In situ tests

Shown in Fig. 6 are the results from the base case in which temperature was varied under zero current conditions. As seen in the close up, a maximum spread of 0.2 ° C was measured between the sensors. This very small offset could be due to the position of the sensors relative to the inlet of the heating water, with FBG1 and the thermocouple being nearest the water inlet.

If the temperature across the cell were indeed uniform, with no gradient induced by the heating system, the data from this baseline would indicate a relative uncertainty between the sensors over the measurement range shown. With this established, any temperature gradients higher than 0.2 ° C during cell operation could be attributed to factors other than the heating system, namely local current flow and associated irreversibilities.

Departure from the baseline case temperature profile was clearly seen while drawing current through the cell at the different cell temperatures. Fig. 7 shows the results of a case where the cell temperature was set to 50 °C. The current was increased from 6 to 12 A allowing the cell voltage to reach steady state in between steps. The most prominent features are the jumps in temperature measured by all the sensors, including the thermocouple; these jumps correlate with each step change in current. The data shows that there is no apparent lag in the response time of the FBGs compared to the thermocouple, which is indicative of their comparable sizes, and location relative to the MEA. In addition, the thermocouple data lies just above FBG1, which is consistent with its physical location and the apparent gradient in temperature across the cell.

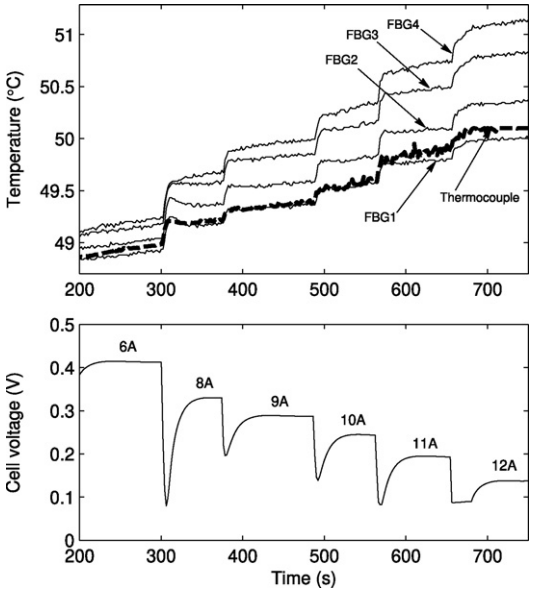

Fig. 7. Time response of FBG and thermocouple (top) with increasing cell current (below). Water temperature for the cell heating system was maintained constant at 50 °C.

An increased in temperature with current draw was expected to be measured by all sensors due primarily to ohmic losses, but gradients across the cell of more than 1 ° C were also observed. Shown in Fig. 8 are the temperatures measured by the FBGs plotted against their location for the same time series of Fig. 7. A positive gradient from inlet to outlet is clearly shown and becomes larger at higher currents indicating a non-uniform current density across the cell. This is consistent with the experimental observations of Wang

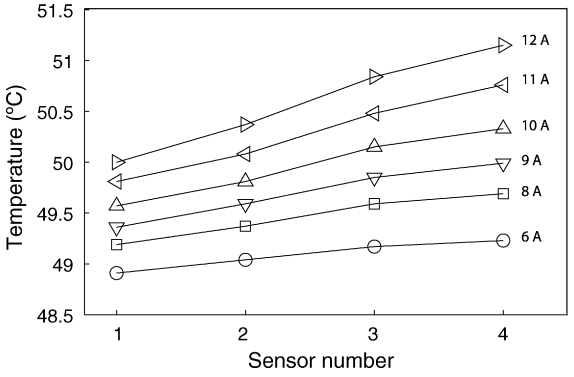

Fig. 8. Temperature profiles for different current densities with cell temperature set near 50 ° C with water heating system.

et al. who attributed this to the improved humidification of the membrane towards the outlet resulting in higher current densities [9].

6. Conclusions

The research presented here demonstrates that FBGs can be embedded inside a PEM fuel cell to reliably measure temperature dynamically with a relative resolution of less than 0.2°. In the interest of improved cell design, this relatively inexpensive technique could prove useful as a diagnostic tool to identify hot spots on the membrane, or as an indirect means of determining current distribution across the cell as done by Wilkinson et al. [6].

Further improvement of the technique will involve the multiplexing of several FBGs on a single fiber. This will increase the number of measurement points from four to upwards of ten resulting in the possibility for truly distributed temperature data within a an operating fuel cell, and the eventual extension of the technique to multi-point monitoring in complete stacks.

Acknowledgements

This work was funded by the Natural Sciences and Engineering Research Council (NSERC) of Canada. Access to the NRC Institute for Fuel Cell Innovation, Vancouver, Canada, and the assistance of Dr. Titichai Navessin in fabricating MEAs is gratefully acknowledged.

References

[1] A. Rowe, X. Li, Journal of Power Sources 102 (2001) 82–96.
[2] N. Djilali, D. Lu, International Journal of Thermal Sciences 41 (2002) 29–40.
[3] A.Z. Weber, J. Newman, Journal of the Electrochemical Society 153 (2006) A2205–A2214.
[4] A. Faghri, Z. Guo, International Journal of Heat and Mass Transfer 48 (2005) 3891–3920.
[5] N. Djilali, Energy 32 (2007) 269–280.
[6] M. Wilkinson, M. Blanco, E. Gu, J.J. Martin, D. Wilkinson, J.J. Zhang, H. Wang, Electrochemical and Solid-State Letters 9 (11) (2006) A507.
[7] S. He, M.M. Mench, S. Tadigadapa, Sensors and Actuators A 125 (2006) 170.
[8] C.-Y. Lee, G.-W. Wu, C.-L. Hsieh, Journal of Power Sources 172 (2007) 363–367.
[9] M. Wang, H. Guo, C. Ma, Journal of Power Sources 157 (2006) 181.
[10] S. Basu, M.W. Renfro, B.M. Cetegen, Journal of Power Sources 162 (2006) 286.
[11] Y.-J. Rao, Measurement Science and Technology 8 (1997) 355–375.